Direct electro-optical pumping for hybrid CdSe nanocrystal/III-nitride based nano-light-emitting diodes

M. Mikulics, Y. C. Arango, A. Winden, R. Adam, A. Hardtdegen, D. Grützmacher, E. Plinski, D. Gregušová, J. Novák, P. Kordoš, A. Moonshiram, M. Marso, Z. Sofer, H. Lüth, and H. Hardtdegen

Citation: Applied Physics Letters **108**, 061107 (2016); doi: 10.1063/1.4941923
View online: http://dx.doi.org/10.1063/1.4941923
View Table of Contents: http://scitation.aip.org/content/aip/journal/apl/108/6?ver=pdfcov
Published by the AIP Publishing

Direct electro-optical pumping for hybrid CdSe nanocrystal/III-nitride based nano-light-emitting diodes

M. Mikulics,[1,2] Y. C. Arango,[1,2] A. Winden,[1,2] R. Adam,[1,2] A. Hardtdegen,[1,2] D. Grützmacher,[1,2] E. Plinski,[3] D. Gregušová,[4] J. Novák,[4] P. Kordoš,[5] A. Moonshiram,[6] M. Marso,[6] Z. Sofer,[7] H. Lüth,[1,2] and H. Hardtdegen[1,2]

[1]*Peter Grünberg Institute, Forschungszentrum Jülich, D-52425 Jülich, Germany*
[2]*Jülich-Aachen Research Alliance, JARA, Fundamentals of Future Information Technology, D-52425 Jülich, Germany*
[3]*Faculty of Electronics, Wroclaw University of Technology, Wybrzeze Wyspianskiego 27, 50-370 Wroclaw, Poland*
[4]*Institute of Electrical Engineering, Slovak Academy of Sciences, SK-84104 Bratislava, Slovak Republic*
[5]*Institute of Electronics and Photonics, Slovak University of Technology, SK-81219 Bratislava, Slovakia*
[6]*Université du Luxembourg - Faculté des Sciences, de la Technologie et de la Communication, Luxembourg, L-1359 Luxembourg*
[7]*Department of Inorganic Chemistry, Institute of Chemical Technology, Technická 5, Prague 6, Czech Republic*

(Received 13 November 2015; accepted 2 February 2016; published online 12 February 2016)

We propose a device concept for a hybrid nanocrystal/III-nitride based nano-LED. Our approach is based on the direct electro-optical pumping of nanocrystals (secondary excitation) by electrically driven InGaN/GaN nano-LEDs as the primary excitation source. To this end, a universal hybrid optoelectronic platform was developed for a large range of optically active nano- and mesoscopic structures. The advantage of the approach is that the emission of the nanocrystals can be electrically induced without the need of contacting them. The proof of principal was demonstrated for the electro-optical pumping of CdSe nanocrystals. The nano-LEDs with a diameter of 100 nm exhibit a very low current of ~8 nA at 5 V bias which is several orders of magnitude smaller than for those conventionally used. The leakage currents in the device layout were typically in the range of 8 pA to 20 pA/cm^2 at 5 V bias. The photon-photon down conversion efficiency was determined to be 27%. Microphotoluminescence and microelectroluminescence characterization demonstrate the potential for future optoelectronics and highly secure "green" information technology applications.
 [http://dx.doi.org/10.1063/1.4941923]

During the last decades, rapid progress in the development of nanostructures brought about new insights into applied physics resulting in a number of new applications for electronics,[1–4] medicine,[5–7] optics or even main stream electronics.[8,9] However it has become more and more challenging on the one hand to connect nanoscale structures to the "real world" and on the other hand to characterize them. There are numerous reasons. The nanostructures consist to a larger part of surface, which is directly exposed to the ambient in the individual technological steps used in conventional device integration. These steps can alter the characteristics of the nanostructures by changing their surface composition.[10] Furthermore, it is quite a challenge to contact non-planar small nanoscale objects.[11,12] At last, the characterization[10,13] of the nanostructures and their altered surfaces is challenging due to the resolution limits of the conventional characterization techniques employed. It becomes ambiguous to relate the characteristics to the properties of "pure," non-surface altered nanostructures. Conventional device concepts have already reached their limits also with respect to the need for reduced energy consumption. The next generation of highly sophisticated optoelectronics based on sub-nanoscale and mesoscopic material systems calls for alternative concepts, which limit processing technology to a minimum, which make contacting superfluous and which can be employed for a large number of different wavelengths and nanoscopic applications. Additionally, they should address the need for low-energy consumption.

Here in our work, we present a device concept based on a direct electro-optical pumping procedure.[14] The device concept constitutes a universal hybrid platform suitable for a large range of materials ranging from atomic through mesoscopic as well as nanometer sized objects. From an application point of view, such a platform should be based on an electrically, physically, and chemically stable and robust material system. III-nitrides with their unique material properties[15,16] were chosen as the best candidate for this purpose. Additionally, their band gaps cover a broad spectral range from ~360 nm (GaN) to ~1700 nm (InN). Here, electrically driven nitride based UV nano-LEDs constitute the primary source for photons, which then serve as an excitation source for single nanocrystals with smaller band gaps. The UV-LEDs generate electron-hole pairs in a large variety of such nanocrystals which then emit at longer wavelengths. Alternative materials such as GaAs can also be employed, but the choice of nanocrystals for secondary emission is then limited. Principally, UV LEDs are already used as excitation sources for nanocrystals such as CdSe[17–19] to obtain white light for solid state lighting.[20–22] Many nanocrystals are electro-optically pumped simultaneously to increase the photon fluxes of the white light. In contrast, our approach aims at extremely low energy consumption optoelectronics by using a nano-LED to excite

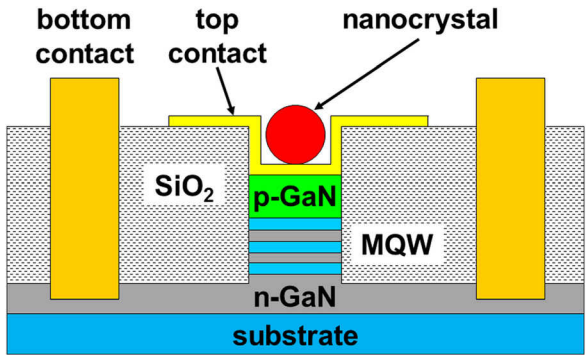

FIG. 1. Principal schematics of the hybrid nanocrystal/III-nitride based nano-LED structure.

just one nanocrystal and to produce *low* photon fluxes and ultimately single photon emission. Even though we realize that there are number of different approaches to obtain single photon emission[23–25] and that colloidal nanocrystals are only limited in their suitability for such an application,[25] CdSe nanocrystals were chosen nevertheless. They are well suited to demonstrate the universal applicability of the hybrid single nanocrystal/III-N based nano-LED approach. The nanocrystals were excited by a (UV) nano-LED. The emission wavelength of the nanocrystals was tuned by utilizing the quantum size effect[26–28] and preparing crystals of the appropriate/desired size. Importantly, the difficult task of direct nanocrystal contacting is circumvented. The hybrid nanocrystal/nano-LED devices were arranged in arrays and are prepared to be singularly addressable in future.[29]

One of the most costly steps in nanostructure processing is e-beam lithography. Our concept calls for only one-time use of e-beam lithography to define the nano-LEDs. All further processing steps are realized with standard optical lithography. In contrast, other device concepts, in which nanostructures are contacted directly, and numerous e-beam lithography steps are employed. Therefore, our concept allows for a reduction of costs since it could significantly increase and simplify the mass production of nanostructured optoelectronic devices. This simple concept is presented in Figure 1.

We started out with an LED structure deposited by metal-organic vapor phase epitaxy (MOVPE) on a 2″ c-plane sapphire substrate using N_2 as the carrier gas[30,31] throughout the deposition of the $In_{0.1}Ga_{0.9}N$ quantum wells and p-GaN layer growth. At first, an n-doped GaN layer with a donor concentration of $5 \times 10^{18}\,cm^{-3}$ was deposited followed by a fivefold quantum well structure (16 nm GaN barrier, 2.5 nm $In_{0.1}Ga_{0.9}N$) which was capped with p and p^{++} GaN with an acceptor concentration of $5 \times 10^{17}\,cm^{-3}$ and $6 \times 10^{18}\,cm^{-3}$, respectively. The fabrication schematics of the hybrid nanocrystal/III nitride based nano-LED technological procedure is presented in Figure 2. At first, nano-LEDs were defined using electron-beam lithography combined with an Ar Ion-Beam-Etching (IBE) process to realize protective Ni-caps according to Figure 2(a) with three different diameters: 100, 150, and 200 nm and with a height of the nano-LED columns of 400–500 nm. This process needs to be optimized carefully[32] since IBE (and also other technological processes[33]) can damage the material and leads to a suppression of radiative recombination. To this end a fast inspection method was used to evaluate the nano-LEDs: microphotoluminescence. No further processing steps are needed. The etching damage is detectable by a decrease of photoluminescence (PL) intensity emitted from etched nanostructures[34] as will be discussed later. All nanostructures were isolated from their neighbors using a hydrogen silsesquioxane (HSQ) thin film, which transforms into SiO_2 upon annealing (Figure 2(b)). The Ni-capping layer was removed by an $HCl:H_2O$ solution (Figure 2(c)). At last, transparent Ni/Au (5/5 nm) top contacts were defined with the help of conventional optical lithography (Figure 2(d)). The entire/analogical technological process was described in detail in a previous publication[35] however with one important exception: the thickness of the spun on HSQ was adjusted so that it does not reach completely up to the top of the Ni cap. This step

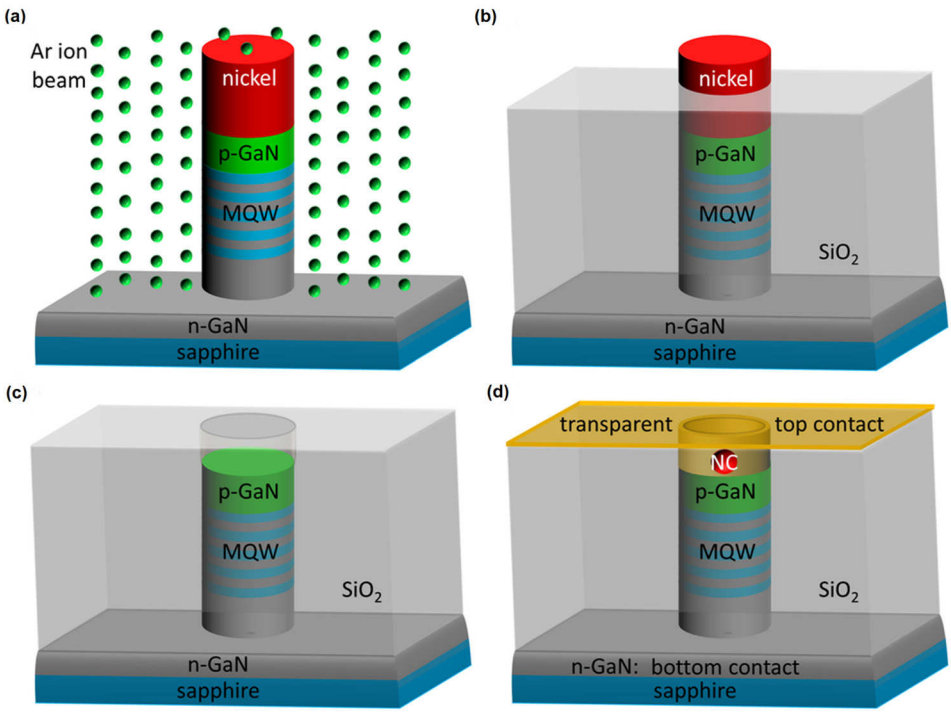

FIG. 2. Fabrication schematics of the hybrid nanocrystal/III nitride based nano-LED (a) after Ar ion beam etching, (b) after encompassing the nanostructures in HSQ/SiO_2 for device insulation, (c) after removal of the protective Ni masking cap, and (d) after formation of transparent top metal contact and nanocrystal integration.

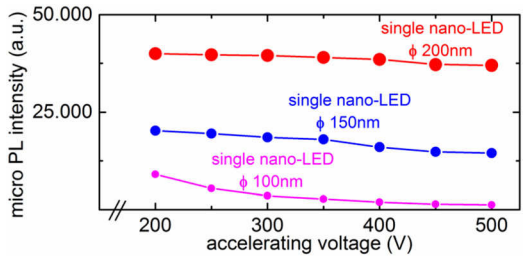

FIG. 3. Micro-PL intensity of nano-LEDs with 100 (pink circles), 150 (blue circles), and 200 (red circles) nm diameter as a function of Ar-IBE accelerating voltage (V_a). The highest intensity is observed for 200 V accelerating voltage which is optimal for nano-LED etching.

is very challenging since an exact control of HSQ thickness during spinning and after annealing has to be ensured. The layer must not cover the Ni-cap but must barely stay below its surface (see Figure 2(b)). A much smaller HSQ thickness was needed for the previous application of nano-LEDs as sources for lithography.[35] After the removal of the Ni cap, an aperture is formed in the SiO_2 (Figure 2(c)), the depth of which (20–100 nm) is tuned with respect to the nanocrystal size chosen. Subsequently, the apertures are conformally covered with the transparent top contact. The nanocrystals fill all the apertures and are in direct contact with the nano-LED (Figure 2(d)).

Figure 3 presents the PL intensity studies for nanostructures of different sizes formed by different Ar-ion accelerating voltages (V_a) during etching. A decrease in accelerating voltage from 500 V to 200 V causes a significant increase in PL intensity emitted by a single nano-LED by ~20% to 300%, as it is evident for all 3 presented nano-LED diameters. In the case of 100 nm nanostructures, a fourfold intensity increase was achieved after etching parameter optimization. We assume that channeling effects as well as surface roughening initialized an increase in non-radiative recombination centers in the region close to the structure "wall." For a small nano-LED diameter, the ratio of "intact" to etch-modified regions plays a more significant role in comparison with large diameter structures. Hence, an optimization of etching parameters needs to be performed more carefully. Furthermore, the PL intensity is primarily influenced by the (nano-LED) volume and increases with size. The intensity is additionally strongly affected by an effective suppression of non-radiative recombination. Figure 4 presents microphotoluminescence spectra for nano-LED structures with 100 and 200 nm in diameter prepared using optimized IBE process parameters. The well-known linear PL peak intensity and energy dependence on structure size[17] are observed. The nanostructures relax in a

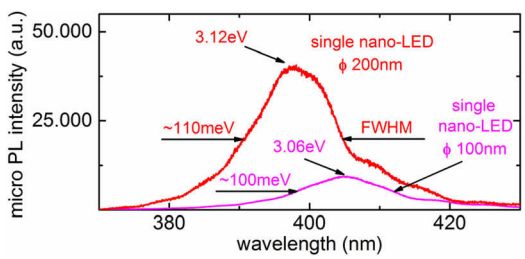

FIG. 4. Micro-PL intensity recorded for nano-LEDs with 100 and 200 nm diameter produced using an optimized Ar-IBE process. The emission wavelength can be tuned by the nano-LED diameter.[35]

size-dependent way due to the Ar-IBE process induced nanostructure formation. A single nano-LED with a diameter of 100 nm exhibits ~60 meV redshift in comparison to its 200 nm etched nanostructure counterpart. This is a reproducible effect can be used to tune the wavelength emission[35] of the primary excitation source.

After the optimization of the nano-LEDs and their integration into a vertical device layout, the fabrication procedure of which was described in detail previously,[35] a universal hybrid optoelectronic platform was prepared for the transfer of CdSe nanocrystals to the optically active top nano-LED area (see schematics–Figure 2(d)). Due to their conical shape caused by the Ar-IBE etching angle, nano-LEDs with a nominal diameter of 100 nm exhibit a diameter at their tops of 50 nm, i.e., the aperture size is ~50 nm (see inset in Figure 6(b)). A conventional chemical preparation approach was used to obtain CdSe colloidal particles and the respective nanocrystals.[36] A commonly used Zetasizer Nano ZS was employed to determine the nanoparticle size distribution in the dispersant. The size centered around 4 nm. In the following, CdSe colloidal particles were dispersed in toluene with a dilution adjusted to fit the aperture density. They were injected onto the top of the nano-LED area. The injection procedure was performed at room temperature by means of a manual micromechanical moving system, similar to our previously reported transfer technique for mesostructures.[37] A quartz-glass micro-pipette with a ~1 μm outer diameter was filled with the CdSe colloidal particle suspension. An area with 50 nm apertures was covered with an about 5 μm droplet of colloidal particle suspension in diameter. After the evaporation of the dispersant, the nanocrystals were found to be randomly distributed across the injected area. Nevertheless, we found crystals in every aperture, i.e., also at the tops of all the nano-LEDs. Figure 5(a) depicts the result of the technological procedure described above. Here we note that a future improvement of the colloidal particle injection technique could increase the technological efficiency as well as the speed of the entire process resulting in a reduction of resources. This is a crucial point for the application of the technique to future mass-production. Figure 5(b) presents the nano-LEDs, for which Ni/Au (5/5 nm) transparent top contacts as well as recessed bottom contacts were fabricated,[35] together with the well-positioned CdSe nanocrystals at their tops. Their integration into a device layout suitable for DC testing and future high frequency (HF) operation is shown in Figure 5(c). The layout was designed and optimized regarding its impedance for a large range of optoelectronic applications using CST Microwave Studio® 2013. For the sake of comparison, equivalent device structures without nano-LEDs were fabricated and tested with the aim of obtaining information on leakage currents. These should be effectively suppressed in order to minimize electrical losses as well as to eliminate heating effects caused by a parasitic current. To this end, the optimization of the HSQ/SiO_2 isolation procedure was carried out.[38,39] DC measurements indicate that the leakage currents in our device layout reached values typically in the range of 8 pA to 20 pA/cm^2 at 5 V bias voltage—the bias level to be used later for nano-LED and direct electro-optic pumping operation.

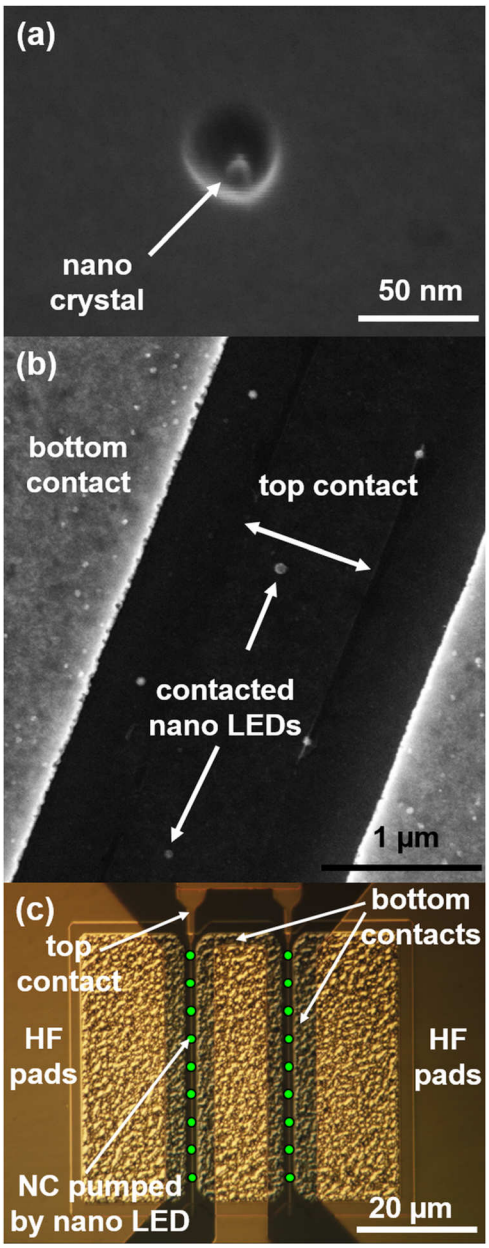

FIG. 5. SEM micrographs: (a) nanocrystal (NC) positioned in SiO_2 hole structure. (b) Array of nano-LEDs with NCs with a transparent Ni/Au (5/5 nm) top contact and annealed Ti/Al/Ni/Au bottom contacts. (c) Fully integrated NC/nano-LED structures (green dots, as a guide to the eye) in the device layout suitable for DC and HF characterization.

In the following, micro-electroluminescence measurements were performed at 5 V bias on selectively contacted nano-LED structures integrated into the vertical device layout. A representative electroluminescence spectrum from a single (100 nm in diameter) nano-LED structure is presented in Figure 6(a). The maximum wavelength emitted from this nano-LED structure is about 402 nm, which corresponds to a photon energy of ~3.08 eV. The I/V characteristic shown in Figure 6(b) indicates a very low energy consumption of ~40 nW at 5 V bias, which may be around 6–7 orders of magnitude lower than for a conventional LED.[40] This emission energy is sufficient to pump/excite CdSe nanocrystals (Figure 5(a)). An example is presented in the inset of Figure 6(c) for a single nanocrystal of ~4 nm in diameter. The nano-LED initiates emission at ~540 nm. The emission wavelength detected is smaller than that for the colloidal nanoparticle dispersion. This is due to the fact that the single nanocrystal excited has a smaller diameter than the mean diameter of the nanocrystals in the dispersion. The emission wavelength of the nanocrystal is also blue-shifted with respect to bulk CdSe. This quantum size effect induced blue shift of the nanocrystal emission wavelength can be exploited for emission wavelength tuning.[26–28] A striking property of the single nanocrystal emission is its spectral sharpness. While the room temperature emission of bulk CdSe is broad, the FWHM of the single CdSe nanocrystal emission peak is only 30 meV. (Even the emission of the colloidal nanoparticles with a certain spread in crystal sizes is considerably sharper (FWHM ~ 140 meV) than observed for bulk CdSe.) For the explanation of this result, the diameter of the excitons in comparison to the CdSe nanocrystal size needs to be taken into account. With the refractive index for CdSe n ~ 3 at 550 nm, the resulting Bohr radius of the excitons amounts to about 4 to 5 nm and is comparable to or even exceeds the nanocrystal size.[28] Consequently, the nanocrystal behaves atom-like and its emission line width becomes extremely sharp. The observed FWHM of 30 meV is most probably due to thermal broadening at room temperature (kT ~ 25 meV at 300 K). The efficiency of the initiated emission for the singular nanocrystal was determined according to previous studies.[41,42] Electroluminescence and photoluminescence emission spectra were integrated and the emission energy of the nano-LED (E_{exc}) and the nanoparticle (E_{emit}) was determined. The ratio E_{emit}/E_{exc} is proportional to the conversion efficiency. The efficiency of photon-photon conversion was calculated to be about 27%. In our case, the electrically driven nano-LED structure emits a train of photons

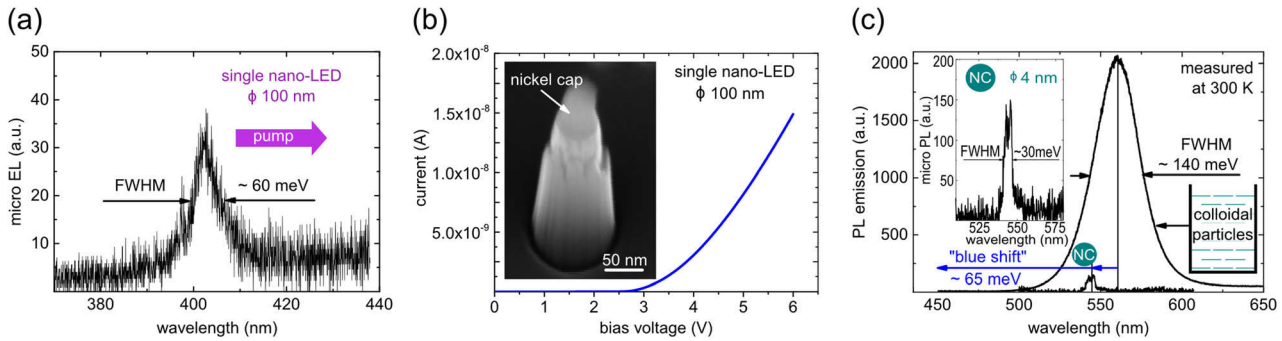

FIG. 6. Micro-EL measurements (a) of a single ø 100 nm nano-LED (pump), (b) I/V characteristic of the respective nano-LED, and (c) micro-PL measurements for CdSe colloidal particles and a single CdSe nanocrystal (NC) with a diameter of ~4 nm (inset). A blue shift of the emission energy by ~65 meV is observed when the dispersant is removed.

with a high energy and number. The photons absorbed by the nanocrystal can only partially be exploited to induce radiative recombination. Since a strong quantum size effect is observed for all nanocrystal sizes studied here, photons with the desired wavelength are emitted just by choosing a suitable nanocrystal size. If the photon counts exceed the maximal photon number absorbable by a single nanocrystal, the quantum efficiency of the whole photon-photon conversion process decreases. However, the photon emission from the primary excitation source—the nano-LED—can be adjusted by the control of current flow. An adequate number of photons can be generated for an efficient quantum conversion in the nanoparticle system. This effect can be utilized to increase the efficiency of the secondary photon emission. The approach constitutes a technology suitable for the mass production of such hybrid photon sources primarily needed for highly secure and reliable communication systems.

In our work, we realized a hybrid nanocrystal/nano-LED devices integrated into a device layout suitable for DC testing and characterization and for future HF operation. The electrically driven nano-LEDs were utilized as the primary excitation sources to directly optically pump emission from the nanoparticles as the secondary sources. The technological procedure of device development and optimization was reported. Quantum size affected emission was observed from the nanoparticles and discussed. The efficiency of photon-photon conversion was calculated to be about 27%. The potential of the hybrid approach to induce single photon emission at a desired wavelength is presented. This universal hybrid optoelectronic platform is suitable for a large range of mesoscopic and nanometer sized applications. Since the nano-LEDs exhibit a very low current of ~8 nA for a diameter of 100 nm at 5 V bias—which may be around 6–7 orders of magnitude smaller than for conventional LEDs[40]—and small leakage currents in the range of 8 pA to 20 pA/cm^2, the device concept is a very promising candidate for a low energy and resources consuming optoelectronics and suitable for mass production.

Y. C. Arango was supported by the Alexander von Humboldt Foundation through a postdoctoral fellowship. Z. Sofer was supported by the Czech Science Foundation (GACR No. 13-20507S). D. Gregušová was supported by the Scientific Grant Agency of Slovak Republic (VEGA No.2/0105/13). J. Novák was supported by the Science and Technology Assistance Agency under Grant No. APVV-14-0297 (Slovak Republic) and by the Scientific Grant Agency of Slovak Republic (VEGA No. 2/0098/13). A. Moonshiram and M. Marso thank the CST A/G, Darmstadt, Germany, for providing the university license for CST Microwave Studio® 2013. H. Lüth thanks A. Pawlis for valuable discussions.

[1]W. Słysz, M. Węgrzecki, J. Bar, P. Grabiec, M. Górska, V. Zwiller, C. Latta, P. Bohi, I. Milostnaya, O. Minaeva, A. Antipov, O. Okunev, A. Korneev, K. Smirnov, B. Voronov, N. Kaurova, G. Gol'tsman, A. Pearlman, A. Cross, I. Komissarov, A. Verevkin, and R. Sobolewski, Appl. Phys. Lett. **88**, 261113 (2006).
[2]C. Thelander, P. Agarwal, S. Brongersma, J. Eymery, L. F. Feiner, A. Forchel, M. Scheffler, W. Riess, B. J. Ohlsson, U. Gösele, and L. Samuelson, Mater. Today **9**, 28 (2006).
[3]K. Tomioka, M. Yoshimura, and T. Fukui, Nature **488**, 189 (2012).
[4]C. M. Natarajan, M. G. Tanner, and R. Hadfield, Supercond. Sci. Technol. **25**, 063001 (2012).
[5]T. Berthing, C. B. Sørensen, J. Nygård, and K. L. Martinez, J. Nanoneurosci. **1**, 3 (2009).
[6]F. Mumm, K. M. Beckwith, S. Bonde, K. L. Martinez, and P. Sikorski, Small **9**, 263 (2013).
[7]R. Elnathan, M. Kwiat, F. Patolsky, and N. H. Voelcker, Nano Today **9**, 172 (2014).
[8]R. Agarwal and C. M. Lieber, Appl. Phys. A **85**, 209 (2006).
[9]M. Mikulics, J. Zhang, J. Serafini, R. Adam, D. Grützmacher, and R. Sobolewski, Appl. Phys. Lett. **101**, 031111 (2012).
[10]S. Rosenthal, J. McBride, S. Pennycook, and L. Feldman, Surf. Sci. Rep. **62**, 111 (2007).
[11]M. S. Gudiksen, K. N. Maher, L. Ouyang, and H. Park, Nano Lett. **5**, 2257 (2005).
[12]D. L. Klein, R. Roth, A. K. L. Lim, A. P. Alivisatos, and P. L. McEuen, Nature **389**, 699 (1997).
[13]P. R. Sajanlal, T. S. Sreeprasad, A. K. Samal, and T. Pradeep, Nano Rev. **2**, 1 (2011).
[14]M. Mikulics and H. Hardtdegen, Germany, 12 December 2012 patent specification DE102012025088 (A1), WO2014094705 A1 (2013).
[15]H. Hardtdegen, N. Kaluza, R. Schmidt, R. Steins, E. V. Yakovlev, R. A. Talalaev, Y. N. Makarov, and J.-T. Zettler, Phys. Status Solidi A **201**, 312 (2004).
[16]S. Chattopadhyay, A. Ganguly, K.-H. Chen, and L.-C. Chen, Crit. Rev. Solid State Mater. Sci. **34**, 224 (2009).
[17]M. A. Schreuder, K. Xiao, I. N. Ivanov, S. M. Weiss, and S. J. Rosenthal, Nano Lett. **10**, 573 (2010).
[18]M. J. Bowers, J. R. McBride, and S. J. Rosenthal, J. Am. Chem. Soc. **127**, 15378 (2005).
[19]S. Chandramohan, B. D. Ryu, H. K. Kim, C.-H. Hong, and E.-K. Suh, Opt. Lett. **36**, 802 (2011).
[20]P. Schlotter, J. Baur, C. Hielscher, M. Kunzer, H. Obloh, R. Schmidt, and J. Schneider, Mater. Sci. Eng. B **59**, 390 (1999).
[21]N. Narendran, N. Maliyagoda, A. Bierman, R. M. Pysar, and M. Overington, Proc. SPIE **3938**, 240–248 (2000).
[22]Q. Dai, C. E. Duty, and M. Z. Hu, Small **6**, 1577 (2010).
[23]P. Munnelly, T. Heindel, M. M. Karow, S. Hofling, M. Kamp, C. Schneider, and S. Reitzenstein, IEEE J. Sel. Top. Quantum Electron. **21**, 1 (2015).
[24]J. A. Smyder and T. D. Krauss, Mater. Today **14**, 382 (2011).
[25]S. Buckley, K. Rivoire, and J. Vučković, Rep. Prog. Phys. **75**, 126503 (2012).
[26]W. W. Yu, L. Qu, W. Guo, and X. Peng, Chem. Mater. **15**, 2854 (2003).
[27]A. L. Stroyuk, A. I. Kryukov, S. Y. Kuchmii, and V. D. Pokhodenko, Theor. Exp. Chem. **41**, 67 (2005).
[28]R. Koole, E. Groeneveld, D. Vanmaekelbergh, A. Meijerink, and C. de Mello Donegá, in *Nanoparticles*, edited by C. de Mello Donega (Springer, Berlin, Heidelberg, 2014), pp. 13–51.
[29]A. Winden, M. Mikulics, D. Grützmacher, and H. Hardtdegen, Nanotechnology **24**, 405302 (2013).
[30]Y. S. Cho, H. Hardtdegen, N. Kaluza, N. Thillosen, R. Steins, Z. Sofer, and H. Lüth, Phys. Status Solidi C **3**, 1408 (2006).
[31]H. Hardtdegen, M. Hollfelder, R. Meyer, R. Carius, H. Münder, S. Frohnhoff, D. Szynka, and H. Lüth, J. Cryst. Growth **124**, 420 (1992).
[32]T. Oikawa, F. Ishikawa, T. Sato, T. Hashizume, and H. Hasegawa, Appl. Surf. Sci. **244**, 84 (2005).
[33]M. Kocan, G. A. Umana-Membreno, F. Recht, A. Baharin, N. A. Fichtenbaum, L. McCarthy, S. Keller, R. Menozzi, U. K. Mishra, G. Parish, and B. D. Nener, Phys. Status Solidi C **5**, 1938 (2008).
[34]M. Mikulics, H. Hardtdegen, D. Gregušová, Z. Sofer, P. Šimek, S. Trellenkamp, D. Grützmacher, H. Lüth, P. Kordoš, and M. Marso, Semicond. Sci. Technol. **27**, 105008 (2012).
[35]M. Mikulics and H. Hardtdegen, Nanotechnology **26**, 185302 (2015).
[36]X. Peng, M. Y. Sfeir, F. Zhang, J. A. Misewich, and S. S. Wong, J. Phys. Chem. C **114**, 8766 (2010).
[37]M. Mikulics, H. Hardtdegen, R. Adam, D. Grützmacher, D. Gregušová, J. Novák, P. Kordoš, Z. Sofer, J. Serafini, J. Zhang, R. Sobolewski, and M. Marso, Semicond. Sci. Technol. **29**, 045022 (2014).
[38]S. Riess, M. Mikulics, A. Winden, R. Adam, M. Marso, D. Grützmacher, and H. Hardtdegen, Jpn. J. Appl. Phys., Part 1 **52**, 08JH10 (2013).
[39]A. Winden, M. Mikulics, A. Haab, D. Grützmacher, and H. Hardtdegen, Jpn. J. Appl. Phys., Part 1 **52**, 08JF05 (2013).
[40]M. Rychetsky, I. L. Koslow, T. Wernicke, J. Rass, V. Hoffmann, M. Weyers, and M. Kneissl, Phys. Status Solidi B **253**, 169–173 (2016).
[41]J. D. Gosnell, M. A. Schreuder, S. J. Rosenthal, and S. M. Weiss, Proc. SPIE **66690**, 66690R–66690R–11 (2007).
[42]L. E. Shea-Rohwer, J. E. Martin, X. Cai, and D. F. Kelley, ECS J. Solid State Sci. Technol. **2**, R3112 (2012).